World Academy of Science, Engineering and Technology
International Journal of Physical and Mathematical Sciences
Vol:8, No:1, 2014

Lattice Boltzmann Simulation of MHD Natural Convection in a Nanofluid-Filled Enclosure with Non-Uniform Heating on Both Side Walls

Imen Mejri, Ahmed Mahmoudi, Mohamed A. Abbassi, Ahmed Omri

***Abstract*—**This paper examines the natural convection in a square enclosure filled with a water-Al_2O_3 nanofluid and is subjected to a magnetic field. The side walls of the cavity have spatially varying sinusoidal temperature distributions. The horizontal walls are adiabatic. Lattice Boltzmann method (LBM) is applied to solve the coupled equations of flow and temperature fields. This study has been carried out for the pertinent parameters in the following ranges: Rayleigh number of the base fluid, $Ra=10^3$ to 10^6, Hartmann number varied from Ha=0 to 90, phase deviation ($\gamma=0$, $\pi/4$, $\pi/2$, $3\pi/4$ and π) and the solid volume fraction of the nanoparticles between Ø = 0 and 6%. The results show that the heat transfer rate increases with an increase of the Rayleigh number but it decreases with an increase of the Hartmann number. For $\gamma=\pi/2$ and $Ra=10^5$ the magnetic field augments the effect of nanoparticles. At Ha=0, the greatest effects of nanoparticles are obtained at $\gamma = 0$ and $\pi/4$ for $Ra=10^4$ and 10^5 respectively.

***Keywords*—**Lattice Boltzmann Method, magnetic field, Natural convection, nanofluid, Sinusoidal temperature distribution.

I. Introduction

THE problem of natural convection in square enclosures has many engineering applications such as: cooling systems of electronic components, building and thermal insulation systems, built-in-storage solar collectors, nuclear reactor systems, food storage industry and geophysical fluid mechanics [1]. Some practical cases such as the crystal growth in fluids, metal casting, fusion reactors and geothermal energy extractions, natural convection is under the influence of a magnetic field [2]-[7]. Khanafer et al. [8] numerically investigated natural convection heat transfer in a two-dimensional vertical enclosure utilizing nanofluids. It was revealed that the heat transfer rate increases with the increase of particle fraction at any given Grashof number. Kahveci [9] numerically studied the heat transfer enhancement of water-based nanofluids in a differentially heated, tilted enclosure for a range of inclination angles, nanoparticle volume fractions, and Rayleigh numbers. It was concluded from the results that suspended nanoparticles substantially increase the heat transfer rate and the average Nusselt number is nearly linear with the increase of solid volume fraction. However, Putra et al. [10] conducted experiments to investigate natural convective heat transfer of aqueous CuO and Al_2O_3 nanofluids inside a cylinder. They observed a systematic and significant deterioration in natural convective heat transfer at Rayleigh numbers from 10^6 to 10^9. The deterioration increased with particle concentration and was more pronounced for CuO nanofluids. Wen and Ding [11] reported that for a Rayleigh number less than 10^6, the natural convection heat transfer rate increasingly decreases with the increase of particle fraction, particularly at low Rayleigh numbers. Pirmohammadi and Ghassemi [12] studied steady laminar natural-convection flow in the presence of a magnetic field in a tilted enclosure heated from below and cooled from top and filled with liquid gallium. They found that for a given inclination angle, as the value of Hartmann number increases, the convection heat transfer is reduced. Furthermore they obtained that at $Ra=10^4$, value of Nusselt number depends strongly on the inclination angle for relatively small values of Hartmann number. Ece and Buyuk [13] examined the steady and laminar natural convection flow in the presence of a magnetic field in an inclined rectangular enclosure heated and cooled on its adjacent walls. They found that the magnetic field suppressed the convective flow and the heat transfer rate. They also showed that the orientation and the aspect ratio of the enclosure and the strength and direction of the magnetic field had significant effects on the flow and temperature fields. Sathiyamoorthy and Chamkha [14] numerically studied natural convection flow of electrically conducting liquid gallium in a square cavity whereas the bottom wall is uniformly heated and the left and right vertical walls are linearly heated while the top wall is kept thermally insulated. They exhibited that the magnetic field with inclined angle has effects on the flow and heat transfer rates in the cavity. Sivasankaran and Ho [15] studied numerically the effects of temperature dependent properties of the natural convection of water in a cavity under the influence of a magnetic field. They showed that the heat transfer rate was influenced by the direction of the external magnetic field and was decreased with an increase of the magnetic field. Wen and Ding [16] investigated the heat transfer enhancement using water–TiO2 nanofluid filled in a rectangular enclosure heated from below. They reported that the natural convection heat transfer rate increasingly decreased with the increase of

Imen Mejri is with Unité de Recherche Matériaux, Energie et Energies Renouvelables (MEER), Faculté des Sciences de Gafsa, B.P.19, Zarroug, Gafsa, 2112, Tunisie (Corresponding author; e-mail: im.mejri85@yahoo.fr).

Ahmed Mahmoudi is with: Unité de Recherche Matériaux, Energie et Energies Renouvelables (MEER), Faculté des Sciences de Gafsa, B.P.19, Zarroug, Gafsa, 2112, Tunisie (e-mail: ahmed.mahmoudi@yahoo.fr).

Mohamed A. Abbassi is with Unité de Recherche Matériaux, Energie et Energies Renouvelables (MEER), Faculté des Sciences de Gafsa, B.P.19, Zarroug, Gafsa, 2112, Tunisie (e-mail: abbassima@gmail.com).

Ahmed Omri is with Unité de Recherche Matériaux, Energie et Energies Renouvelables (MEER), Faculté des Sciences de Gafsa, B.P.19, Zarroug, Gafsa, 2112, Tunisie (e-mail: ahom206@yahoo.fr).

particle concentration, particularly at low Rayleigh number. Oztop and Abu-Nada [17] studied the effects of a partial heater on natural convection using different types and concentrations of nanoparticles. They found that heat transfer was strongly related to types and volume fractions of nanoparticles. Abu-Nada [18], [19] and Abu-Nada et al. [20] studied the effect of the variables properties of nanofluids in natural convection. They related the deterioration in heat transfer of nanofluids in natural convection to the temperature dependence of nanofluid properties. These findings were also supported by other studies [21], [22]. Alam et al. [23] investigated natural convection in a rectangular enclosure due to partial heating and cooling at vertical walls. Fattahi et al. [24] applied Lattice Boltzmann Method to investigate the natural convection flows utilizing nanofluids in a square cavity. The fluid in the cavity was a water-based nanofluid containing Al_2O_3 or Cu nanoparticles. The results indicated that by increasing solid volume fraction, the average Nusselt number increased for both nanofluids. It was found that the effects of solid volume fraction for Cu were stronger than Al_2O_3. Kefayati et al. [25] simulated by the Lattice Boltzmann method the natural convection in enclosures using water/SiO_2 nanofluid. The results showed that the average Nusselt number increased with volume fraction for the whole range of Rayleigh numbers and aspect ratios. Also the effect of nanoparticles on heat transfer augmented as the enclosure aspect ratio increased. Lai and Yang [26] performed mathematical modeling to simulate natural convection of Al_2O_3/water nanofluids in a vertical square enclosure using the Lattice Boltzmann method. The results indicated that the average Nusselt number increased with the increase of Rayleigh number and particle volume concentration. The average Nusselt number with the use of nanofluid was higher than the use of water under the same Rayleigh number. Mahmoudi et al. [27] presented a numerical study of natural convection cooling of two heat sources vertically attached to horizontal walls of a cavity. The results indicated that the flow field and temperature distributions inside the cavity were strongly dependent on the Rayleigh numbers and the position of the heat sources. The results also indicated that the Nusselt number was an increasing function of the Rayleigh number, the distance between two heat sources, and distance from the wall and the average Nusselt number increased linearly with the increase in the solid volume fraction of nanoparticles. Kefayati et al. [28] investigated Prandtl number effect on natural convection MHD in an open cavity which has been filled respectively with liquid gallium, air and water by Lattice Boltzmann Method. They exhibited that heat transfer declines with the increment of Hartmann number, while this reduction is marginal for $Ra=10^3$ by comparison with other Rayleigh numbers. Lattice Boltzmann Method simulation of MHD mixed convection in a lid-driven square cavity with linearly heated wall is investigated by Kefayati et al. [29]. It was demonstrated that the augmentation of Richardson number causes heat transfer to increase, as the heat transfer decreases by the increment of Hartmann number for various Richardson numbers and the directions of the magnetic field. The LBM is an applicable method for simulating fluid flow and heat transfer [30]-[34]. This method was also applied to simulate the MHD [35] and, recently, nanofluid [36] successfully.

The aim of the present study is to identify the ability of Lattice Boltzmann Method (LBM) for solving nanofluid, magnetic field simultaneously in the presence of a sinusoidal boundary condition. Moreover, the effects of magnetic field and phase deviations on the heat transfer in the cavity. In fact, it is endeavored to express the best situation for heat transfer and fluid flow with the considered parameters. Hence, the Al_2O_3–water nanofluid on laminar natural convection heat transfer at the presence of a magnetic field in sinusoidal temperature distribution on vertical side walls of the cavity by LBM was investigated.

II. Mathematical Formulation

A. Problem Statement

A two-dimensional square cavity is considered for the present study with the physical dimensions as shown in Fig. 1. The side walls of the cavity have spatially varying sinusoidal temperature distributions. The horizontal walls are adiabatic. The cavity is filled with water and Al_2O_3 nanoparticles. The nanofluid is Newtonian and incompressible. The flow is considered to be steady, two dimensional and laminar, and the radiation effects are negligible. The thermo-physical properties of the base fluid and the nanoparticles are given in Table I. The density variation in the nanofluid is approximated by the standard Boussinesq model. The magnetic field strength B_0 is applied in the horizontal direction. It is assumed that the induced magnetic field produced by the motion of an electrically conducting fluid is negligible compared to the applied magnetic field. Furthermore, it is assumed that the viscous dissipation and Joule heating are neglected.

Therefore, governing equations can be written in dimensional form as follows:

$$\frac{\partial u}{\partial x}+\frac{\partial v}{\partial y}=0 \tag{1}$$

$$\rho_{nf}\left(u\frac{\partial u}{\partial x}+v\frac{\partial u}{\partial y}\right)=-\frac{\partial p}{\partial x}+\mu_{nf}\left(\frac{\partial^2 u}{\partial x^2}+\frac{\partial^2 u}{\partial y^2}\right) \tag{2}$$

$$\rho_{nf}\left(u\frac{\partial v}{\partial x}+v\frac{\partial v}{\partial y}\right)=-\frac{\partial p}{\partial y}+\mu_{nf}\left(\frac{\partial^2 v}{\partial x^2}+\frac{\partial^2 v}{\partial y^2}\right)+F_y \tag{3}$$

$$u\frac{\partial T}{\partial x}+v\frac{\partial T}{\partial y}=\alpha_{nf}\left(\frac{\partial^2 T}{\partial x^2}+\frac{\partial^2 T}{\partial y^2}\right) \tag{4}$$

where F_y is the total body forces at y direction and it is defined as follows:

$$F_y=-\frac{Ha^2\mu_{nf}}{H^2}v+(\rho\beta)_{nf}\,g(T-T_m) \tag{5}$$

where Ha is

$$Ha = HB_0\sqrt{\frac{\sigma_{nf}}{\mu_{nf}}}$$

The classical models reported in the literature are used to determine the properties of the nanofluid [37]:

$$\rho_{nf} = (1-\phi)\rho_f + \phi\rho_p \tag{6}$$

$$(\rho c_p)_{nf} = (1-\phi)(\rho c_p)_f + \phi(\rho c_p)_p \tag{7}$$

$$(\rho\beta)_{nf} = (1-\phi)(\rho\beta)_f + \phi(\rho\beta)_p \tag{8}$$

$$\alpha_{nf} = \frac{k_{nf}}{(\rho c_p)_{nf}} \tag{9}$$

In the above equations, ϕ is the solid volume fraction, ρ is the density, σ is the electrical conductivity, α is the thermal diffusivity, c_p is the specific heat at constant pressure and β is the thermal expansion coefficient of the nanofluid, γ is the phase deviation. The effective dynamic viscosity and thermal conductivity of the nanofluid can be modelled by [38], [39]:

$$\mu_{nf} = \frac{\mu_f}{(1-\phi)^{2.5}} \tag{10}$$

$$k_{nf} = k_f\frac{k_P + 2k_f - 2\phi(k_f - k_P)}{k_P + 2k_f + \phi(k_f - k_P)} \tag{11}$$

The governing equations are subject to the following boundary conditions:

Bottom wall $u = v = 0 \quad \left.\frac{\partial T}{\partial y}\right|_{y=0} = 0$

Top wall $u = v = 0 \quad \left.\frac{\partial T}{\partial y}\right|_{y=H} = 0$ (12)

Left wall $u = v = 0 \quad T(0,y) = T_C + A_l\sin(2\pi y/H)$

Right wall $u = v = 0 \quad T(H,y) = T_C + A_r\sin(2\pi\frac{y}{H} + \gamma)$

B. Simulation of MHD and Nanofluid with LBM

For the incompressible non isothermal problems, Lattice Boltzmann Method (LBM) utilizes two distribution functions, *f* and *g*, for the flow and temperature fields respectively.

For the flow field:

$$f_i\left(\mathbf{x}+\mathbf{c_i}\Delta t, t+\Delta t\right) = f_i\left(\mathbf{x},t\right) - \frac{1}{\tau_v}\left(f_i\left(\mathbf{x},t\right) - f_i^{\mathrm{eq}}\left(\mathbf{x},t\right)\right) + \Delta t F_i \tag{13}$$

For the temperature field:

$$\mathrm{g}_i\left(\mathbf{x}+\mathbf{c_i}\Delta t, t+\Delta t\right) = \mathrm{g}_i\left(\mathbf{x},t\right) - \frac{1}{\tau_\alpha}\left(\mathrm{g}_i\left(\mathbf{x},t\right) - \mathrm{g}_i^{\mathrm{eq}}\left(\mathbf{x},t\right)\right) \tag{14}$$

where the discrete particle velocity vectors defined by $\mathbf{c_i}$, Δt denotes lattice time step which is set to unity. τ_v, τ_α are the relaxation time for the flow and temperature fields, respectively. $f_i^{\mathrm{eq}}, \mathrm{g}_i^{\mathrm{eq}}$ are the local equilibrium distribution functions that have an appropriately prescribed functional dependence on the local hydrodynamic properties which are calculated with (15) and (16) for flow and temperature fields respectively.

$$f_i^{\mathrm{eq}} = \omega_i\rho\left[1 + \frac{3(\mathbf{c_i}.\mathbf{u})}{c^2} + \frac{9(\mathbf{c_i}.\mathbf{u})^2}{2c^4} - \frac{3\mathbf{u}^2}{2c^2}\right] \tag{15}$$

$$\mathrm{g}_i^{\mathrm{eq}} = \omega_i' T\left[1 + 3\frac{\mathbf{c_i}.\mathbf{u}}{c^2}\right] \tag{16}$$

u and ρ are the macroscopic velocity and density, respectively. *c* is the lattice speed which is equal to $\Delta x/\Delta t$ where Δx is the lattice space similar to the lattice time step Δt which is equal to unity, ω_i is the weighting factor for flow, ω_i' is the weighting factor for temperature. D2Q9 model for flow and D2Q4 model for temperature are used in this work so that the weighting factors and the discrete particle velocity vectors are different for these two models and they are calculated with (17)-(19) as follows:

For D2Q9:

$$\omega_0 = \frac{4}{9}, \omega_i = \frac{1}{9} \text{ for i} = 1,2,3,4 \text{ and } \omega_i = \frac{1}{36} \text{ for i} = 5,6,7,8 \tag{17}$$

$$\mathbf{c_i} = \begin{cases} 0 & i = 0 \\ \begin{cases} c(\cos[(i-1)\pi/2]) \\ c(\sin[(i-1)\pi/2]) \end{cases} & i = 1,2,3,4 \\ \begin{cases} \sqrt{2}c(\cos[(i-5)\pi/2+\pi/4]) \\ \sqrt{2}c(\sin[(i-5)\pi/2+\pi/4]) \end{cases} & i = 5,6,7,8 \end{cases} \tag{18}$$

For D2Q4:

The temperature weighting factor for each direction is equal to $\omega_i' = 1/4$.

$$\mathbf{c_i} = (\cos[(i-1)\pi/2], \sin[(i-1)\pi/2])c \quad i = 1,2,3,4 \tag{19}$$

The kinematic viscosity *v* and the thermal diffusivity α are then related to the relaxation time by (20):

$$v = \left[\tau_v - \frac{1}{2}\right]c_s^{\,2}\Delta t \qquad \alpha = \left[\tau_\alpha - \frac{1}{2}\right]c_s^{\,2}\Delta t \tag{20}$$

where c_s is the lattice speed of sound witch is equals to $c_s = c/\sqrt{3}$. In the simulation of natural convection, the external force term *F* appearing in (14) is given by (21)

$$F_i = \frac{\omega_i}{c_s^2} F.c_i \tag{21}$$

where $F = F_y$

The macroscopic quantities, **u** and *T* can be calculated by the mentioned variables, with (22)-(24).

$$\rho = \sum_i f_i \tag{22}$$

$$\rho \mathbf{u} = \sum_i f_i \mathbf{c_i} \tag{23}$$

$$T = \sum_i g_i \tag{24}$$

C. Boundary Conditions

The implementation of boundary conditions is very important for the simulation. The distribution functions out of the domain are known from the streaming process. The unknown distribution functions are those toward the domain.

For Flow:

Bounce-back boundary conditions were applied on all solid boundaries, which mean that incoming boundary populations are equal to out-going populations after the collision.

For Temperature:

The bounce back boundary condition is used on the adiabatic wall. Temperature at the left and the right walls are known. Since we are using D2Q4, the unknown internal energy distribution functions are evaluated as:

Right wall: $$g_3 = T(y) - g_1 - g_2 - g_4 \tag{25}$$

Left wall: $$g_1 = T(y) - g_2 - g_3 - g_4 \tag{26}$$

D. Non Dimensional Parameters

By fixing Rayleigh number, Prandtl number and Mach number, the viscosity and thermal diffusivity are calculated from the definition of these non dimensional parameters.

$$\nu_f = N.Ma.c_s\sqrt{\frac{\mathrm{Pr}}{\mathrm{Ra}}} \tag{27}$$

where *N* is number of lattices in y-direction. Rayleigh and Prandtl numbers are defined as: $Ra = \frac{g\beta_f H^3 (T_h - T_c)}{\nu_f \alpha_f}$ and $\mathrm{Pr} = \frac{\nu_f}{\alpha_f}$, respectively. Mach number should be less than $Ma = 0.3$ to insure an incompressible flow. Therefore, in the present study, Mach number was fixed at $Ma = 0.1$. Nusselt number is one of the most important dimensionless parameters in the description of the convective heat transport. The local Nusselt number (Nul and Nur), the average Nusselt number (Nu) and the dimensionless average Nusselt number (Nu*) are calculated as:

$$\mathrm{Nul} = -\frac{k_{nf}}{k_f}\frac{H}{\mathrm{T_h} - \mathrm{T_c}}\left.\frac{\partial T}{\partial x}\right|_{x=0} \tag{28}$$

$$\mathrm{Nur} = -\frac{k_{nf}}{k_f}\frac{H}{\mathrm{T_h} - \mathrm{T_c}}\left.\frac{\partial T}{\partial x}\right|_{x=H} \tag{29}$$

$$\mathrm{Nu} = \frac{1}{H}\int_{heating\ half} \mathrm{Nur}\ dy + \frac{1}{H}\int_{heating\ half} \mathrm{Nul}\ dy \tag{30}$$

$$\mathrm{Nu}^*(\phi) = \frac{\mathrm{Nu}(\phi)}{\mathrm{Nu}(\phi = 0)} \tag{31}$$

III. Validation of the Numerical Code

Lattice Boltzmann Method scheme was utilized to obtain the numerical simulations in a cavity with a sinusoidal boundary condition that is filled with nanofluid of water/Al_2O_3. Fig. 2 demonstrates the effect of grid resolution and the lattice sizes (20x20), (40x40), (60x60), (80x80) and (100x100) for Ha=0 and $\phi = 0$ by calculating the average Nusselt number for Ra=10^3 and 10^5, it was found that a grid size of (100x100) ensures a grid independent solution. In order to check on the accuracy of the numerical technique employed for the solution of the considered problem, the present numerical code was validated with the published study of Deng et al. [40] for the same cavity with sinusoidal boundary conditions for $\gamma = \pi/2$, Ra=10^5 and Pr=0.7. The results are presented in Fig. 3 as streamlines and isotherms have a good agreement between both compared methods. Another validation with results by Ghasemi et al. [41] at the presence of nanofluid and magnetic field is represented in Fig. 4 it shows the dimensionless temperature along the horizontal axial midline of the enclosure for three values of the Hartmann number, for Ra=10^5 and for a solid volume fraction ϕ= 0.03, excellent agreement is also found. The present code is also validated with the results of Khanafer et al. [8] and Jahanshahiet al. [42] for natural convection in an enclosure filled with water/Cu nanofluid for Ra=6.2x10^5 and ϕ =0.1 as shown in Fig. 5 based on the aforementioned comparisons, the developed code is reliable for studying natural convection in nanofluid subjected to a magnetic field.

IV. Results and Discussion

Figs. 6 and 7 illustrate the effect of Hartmann number for different values of the Rayleigh number (Ra = 10^3, 10^4, 10^5 and 10^6) and for $\gamma = \pi/2$ on the isotherms and streamlines of

nanofluid (ϕ=0.04) and pure fluid (ϕ=0). For all Rayleigh number it demonstrates that the effect of nanoparticles on the isotherms decreases with the augmentation of Hartmann number. The thickness of the boundary layer decreases with the rise of Hartmann number and it results in decrease in heat transfer by the magnetic field (Fig. 8 (a)) shows the variation of average Nusselt number as function of Hartmann number for different Rayleigh number, the increase of Rayleigh number increases the heat transfer rate, on the contrary, the increase of the Hartmann decreases the heat transfer rate. The streamlines shows that the flow behavior is affected with the change in the Rayleigh number and the Hartmann number. At Ra = 10^3-10^4 and in the absence of magnetic field, the flow is characterized by two cells, one above the other, rotating in opposite direction inside the enclosure. The minor cell near the let-top corner is elongated when the Hartmann number is increased to 30 and 60 and when Rayleigh number is increased to 10^5 and 10^6 also a third cell appears near the right-bottom corner. The strength of these cells increases as the Rayleigh number increases and decreases as the Hartmann number increases. For all values of Rayleigh number, the application of the magnetic field has the tendency to slow down the movement of the fluid in the enclosure. The braking effect of the magnetic field is observed from the maximum intensity of circulation $|\psi|_{max}$ (Fig. 8 (b)) presents the variation of the maximum value of the stream function as a function of Hartman number for several values of Rayleigh number for ϕ =0 and γ =π/2. It is observed that the effect of Hartmann number is opposite to the effect of Rayleigh number. For Ra = 10^3 and 10^4, $|\psi|_{max}$ is constant and small for all values of Hartmann number. The conduction is dominant. For Ra = 10^5 and 10^6, the convection is dominant for low values of Hartmann number, more than the Hartmann number increases convection is more disadvantaged, until reaching the conductive regime.

Figs. 9 (a) and (b) illustrate the variations of the local Nusselt numbers along the left sidewall and right sidewall at various Rayleigh numbers for Ha=0 and 60. For both walls, the curves drawn for the Nusselt numbers against y/H are approximately of sinusoidal shape like the thermal boundary. This indicates that the local heat transfer is directly affected by the temperature distribution on the surface. In other words, larger heat transfer occurs when the temperature is higher. In the left sidewall, it is obviously understood that the lower half (0 $\leq$y/H$\leq$ 0.5) is the heating half and the upper half (0.5 $\leq$y/H$\leq$1) is the cooling half. The variations of the local Nusselt numbers along the left sidewall and the right sidewall are exhibited in Figs. 10 (a) and (b) for various Hartmann numbers. At Ra$\leq 10^4$ the heat transfer gets no remarkable change on both sidewalls even if the Hartmann number is increased but for 10^4<Ra$\leq 10^6$ it seems that the Nusselt number decreases while the Hartmann number is increased.

Fig. 11 shows comparison of the average Nusselt number and the dimensionless average Nusselt number for various Hartmann and Rayleigh numbers at different volume fractions for γ=π/2. The average Nusselt number demonstrates that heat transfer increases with the enhancement of Hartmann number at Ra=10^3. For 10^4 heat transfer declines with the enhancement of Hartmann number from Ha=0 to 30 but the average Nusselt number of Ha=90 is more than Ha=60. Indisputably, the best parameter for showing the effect of the addition of nanopaticles to the pure fluid is the dimensionless average Nusselt number. At Ra=10^3, the best effect of nanoparticles is obtained for Ha = 0, by increasing the Hartmann number the effect of nanoparticles decreases. At Ra=10^4 the lowest effect of nanoparticles is obtained for Ha = 0, for Ha=30-90 the nanoparticles have the same tendency to the increase of the solid volume fraction. At Ra=10^4 the lowest effect of nanoparticles is obtained for Ha = 0, for Ha=30-90 the nanoparticles have the same tendency to the increase of the heat transfer. At Ra=10^5, the augmentation of Hartmann number play a positive role in the improvement of nanoparticles effect on heat transfer albeit the tendency ceases from Ha=60 to 90.

Figs. 12 (a) and (b) indicate the local Nusselt number on the right and left sidewalls for various volume fractions at Ra=10^5, γ=π/2 and Ha=0-90. It is shown that the effect of nanoparticles is more significant for Ha = 90 which is consistent with Fig. 11.

Figs. 13 and 14 illustrate the effect of Rayleigh number (Ra=10^3,10^4 and 10^5) for different phase deviation (γ = 0, π/4, 3π/2 and π) and for Ha=0 on the isotherms and streamlines of nanofluid (ϕ=0.04) and pure fluid (ϕ=0). It shown the isotherms along the left sidewall are retained. Hence, the heat transfer on the left sidewall is kept fixed, but that on the right sidewall is varied. At γ = 0, for Ra<10^5 four cells are formed with approximately symmetries about middle of the cavity, for Ra=10^5 symmetry is broken only for ϕ=0. As the phase deviation increases up to γ = π/4, a multi-cellular flow structure is formed in the cavity with one large diagonal cell and two smaller corner cells. As the phase deviation increases, the size of the upper left-corner cell is enlarged but the lower right-corner cell disappears. At γ = π, the flow structure is of two identical cells in the enclosure.

Figs. 15 (a) and (b) show the effect of the phase deviation for Ra=10^3 and 10^5 on the local Nusselt number along the y coordinates of the two vertical sidewalls at ϕ=0 and Ha=0. At Ra=10^3 it is observed that the heat transfer of the left wall is not affected so much on changing the phase deviation, but the heat transfer of the right wall is affected significantly on changing the phase deviation from γ = 0 to π. The local Nusselt number curves are approximately of sinusoidal shape like the thermal boundary along the vertical walls. This clearly shows that the local heat transfer is directly affected by the temperature distribution on the surface. It is also found that a higher heat transfer occurs where the temperature is higher. At Ra=10^5 the local Nusselt number along the right side wall is greatly affected by changing the phase deviation. It is also found that the local Nusselt number is increased as the Rayleigh number increases.

Fig. 16 shows the effects of volume fractions and phase deviations for various Rayleigh numbers on the average

Nusselt number and the dimensionless average Nusselt number. For all Rayleigh number and phase deviations the heat transfer increases with the rise of volume fraction. For $Ra=10^3$heat transfer decreases from $\gamma= 0$ to $\pi/4$ and increases from $\gamma = \pi/2$ to π. Moreover, the dimensionless average Nusselt number has the same trend in different phase deviations. The nanofluids have effects very similar for all phase deviations. At $Ra =10^4$ and 10^5 heat transfer increases with the rise of phase deviations, the most heat transfer was obtained in $\gamma = \pi$. the best effect of nanoparticles for $Ra =10^4$ and 10^5 is obtained in $\gamma = 0$ and $\pi/4$ respectively.

Fig. 17 shows the effect of nature of nanoparticles on heat transfer. Three nanoparticles are compared at $Ra =10^5$, Ha=0 and $\gamma=\pi/2$. The heat transfer depends strongly on the nano thermal conductivity, so water-Cu nanofluid enhances the heat transfer compared with water-Al_2O_3 and water-TiO_2. Table I shows the proportionally to the solid volume fraction.

V. CONCLUSION

In this paper the effects of a magnetic field on nanofluid flow in a cavity with a sinusoidal boundary condition has been analyzed with Lattice Boltzmann Method. This study has been carried out for the pertinent parameters in the following ranges: the Rayleigh number of base fluid, $Ra=10^3–10^6$, Hartmann number of the magnetic field between 0 and 90, the volume fraction is from ϕ=0 to 0.06 and the direction of the phase deviation (γ=0, $\pi/4$, $\pi/2$, $3\pi/4$ and π). This investigation was performed for various mentioned parameters and some conclusions were summarized as follows:

- A good agreement valid with previous numerical investigations demonstrates that Lattice Boltzmann Method is an appropriate method for different applicable problems.
- for $\gamma = \pi/2$, heat transfer and fluid flow decline with increase in Hartmann number and increase with increase Rayleigh number.
- At $\gamma = \pi/2$, the growth of nanoparticles volume fraction improves heat transfer for Hartmann number from Ha=0 to 90 and for Rayleigh number from $Ra=10^3$ to 10^5. For $Ra=10^5$ the most effect of nanoparticles is obtained for Ha=90.
- For all phase deviations the growth of nanoparticles volume fraction improves heat transfer. At $Ra=10^5$ and Ha=0 the heat transfer rate increases with the rise of phase deviations, the most effect of nanoparticles is obtained for $\gamma=\pi/4$.

TABLE I
THERMO-PHYSICAL PROPERTIES OF WATER AND NANOPARTICLES

	ρ (kg /m^3)	C_p (J/kg K)	K (W/mK)	β (K^{-1})
Pure water	997.1	4179	0.613	$21x10^{-5}$
Al_2O_3	3970	765	40	$0.85x10^{-5}$
Cu	8933	385	400	$1.67x10^{-5}$
TiO_2	4250	686.2	8.9538	$0.9x10^{-5}$

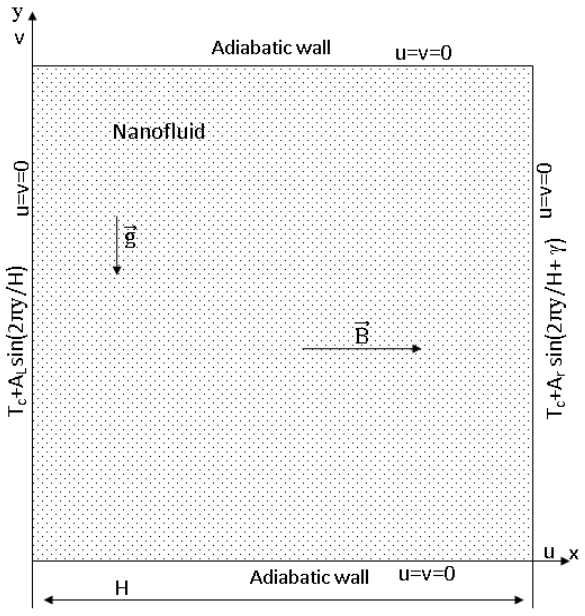

Fig. 1 Geometry of the present study with boundary conditions

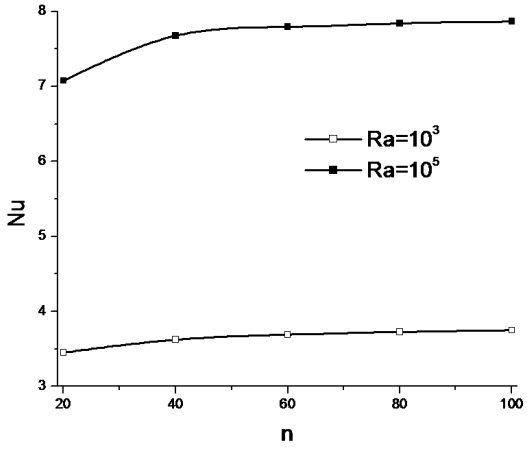

Fig. 2 Average Nusselt number for different uniform grids ($\phi = 0$, $\gamma=\pi/2$ and Ha=0)

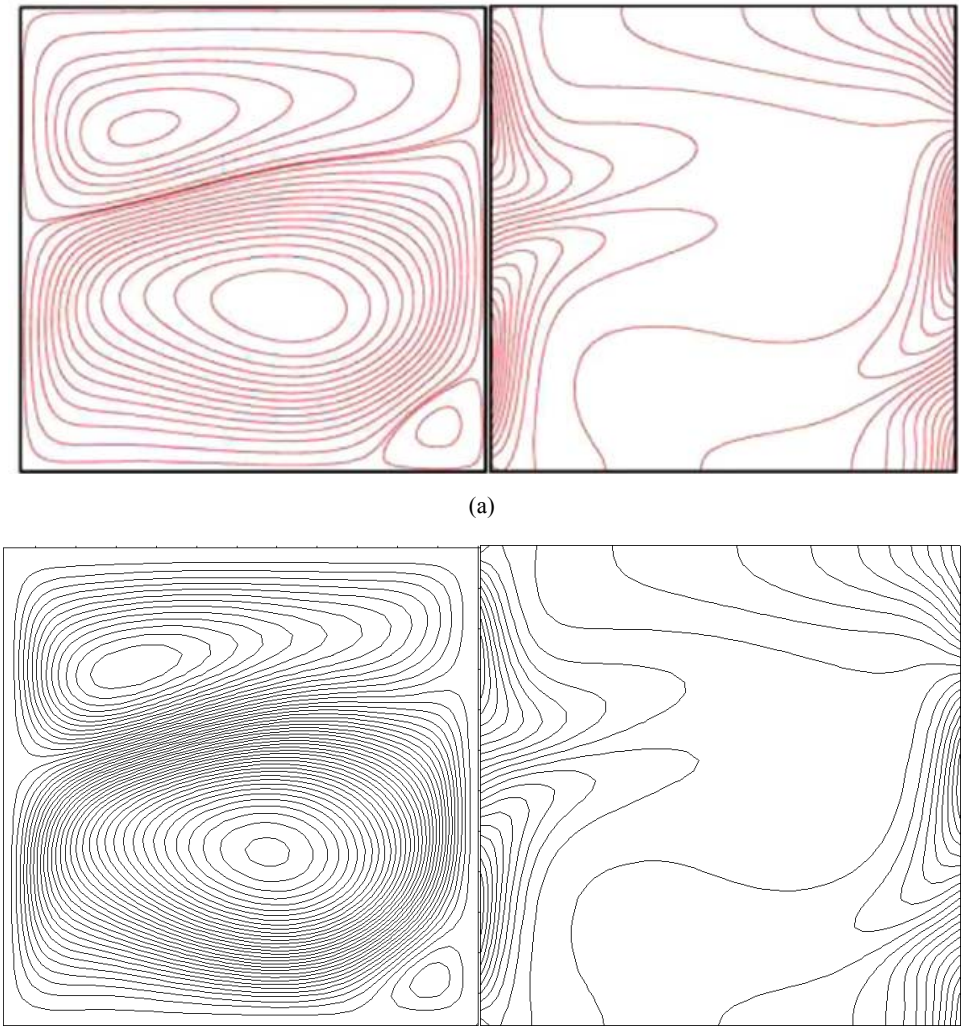

(a)

(b)

Fig. 3 Comparison of the streamlines and isotherms for Ra=10^5 and Pr = 0.7 between (a) numerical results by Deng et al. [40] and (b) the present result

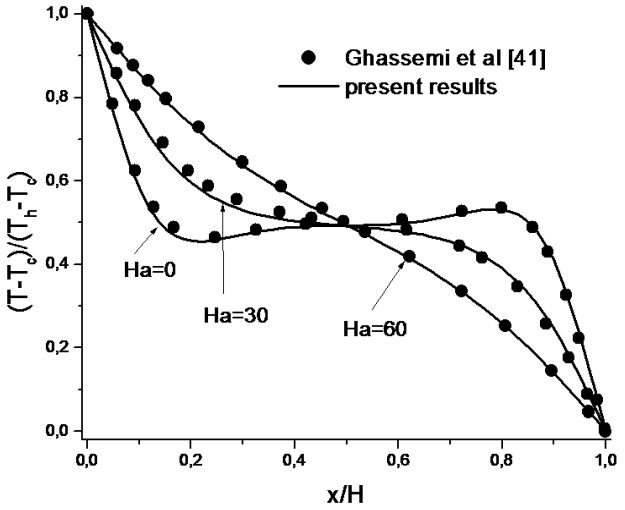

Fig. 4 Comparison of the temperature on axial midline between the present results and numerical results by Ghassemi et al. [8] ($\phi = 0.03$, Ra=10^5)

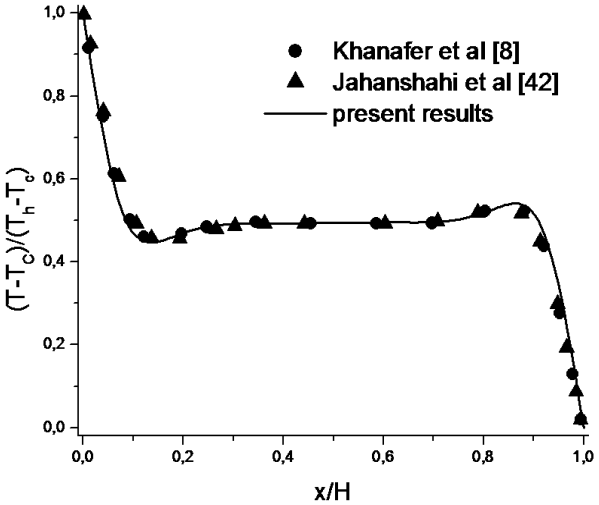

Fig. 5 Comparison of the temperature on axial midline between the present results and numerical results by Khanafer et al. [8] and Jahanshahi et al. [42] (Pr = 6.2, $\phi = 0.1$, Gr = 10^4)

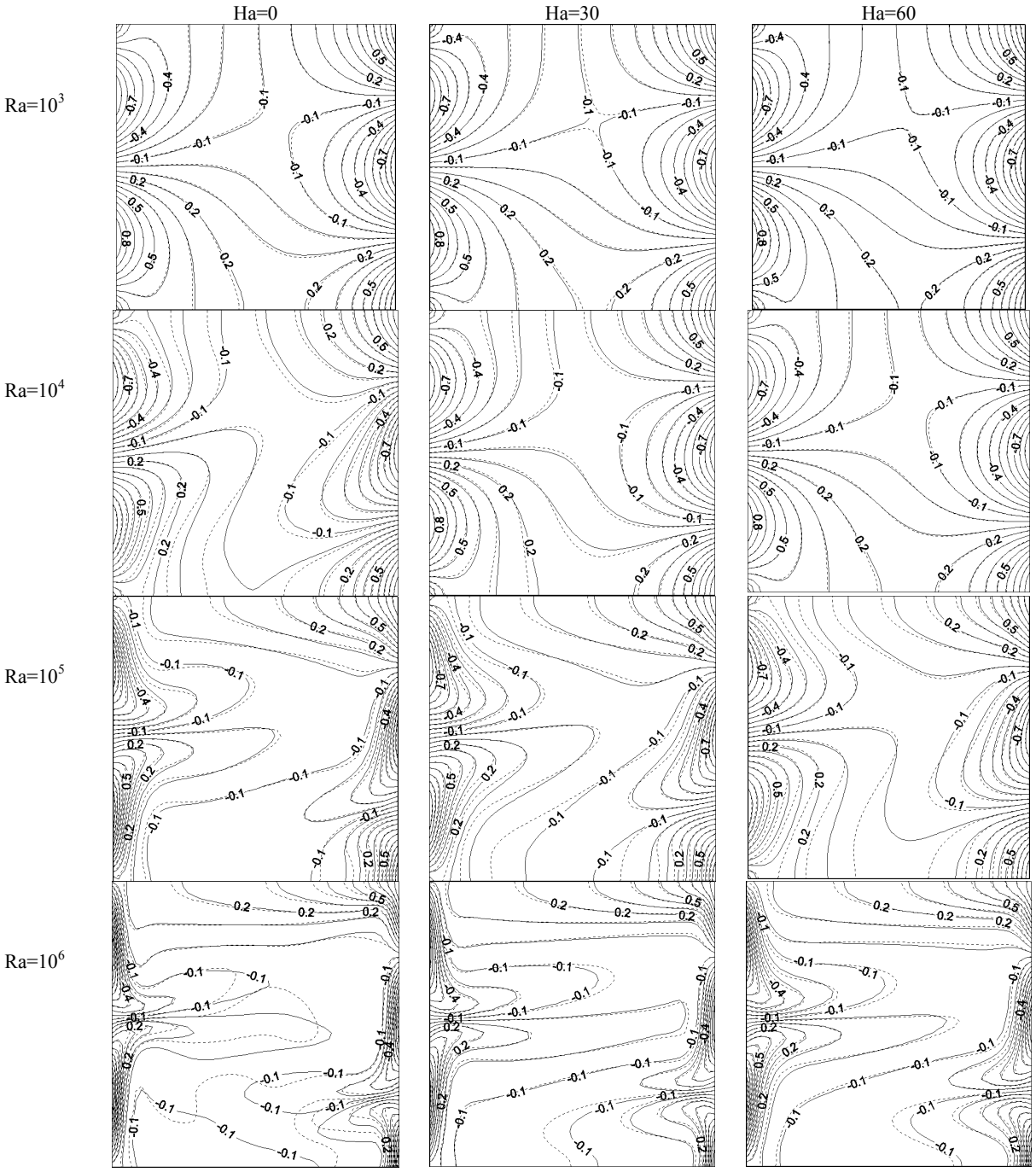

Fig. 6 Isotherms for different Hartmann and Rayleigh numbers and for γ=π/2, (—) $\phi = 0.04$ and (- - -) $\phi = 0$

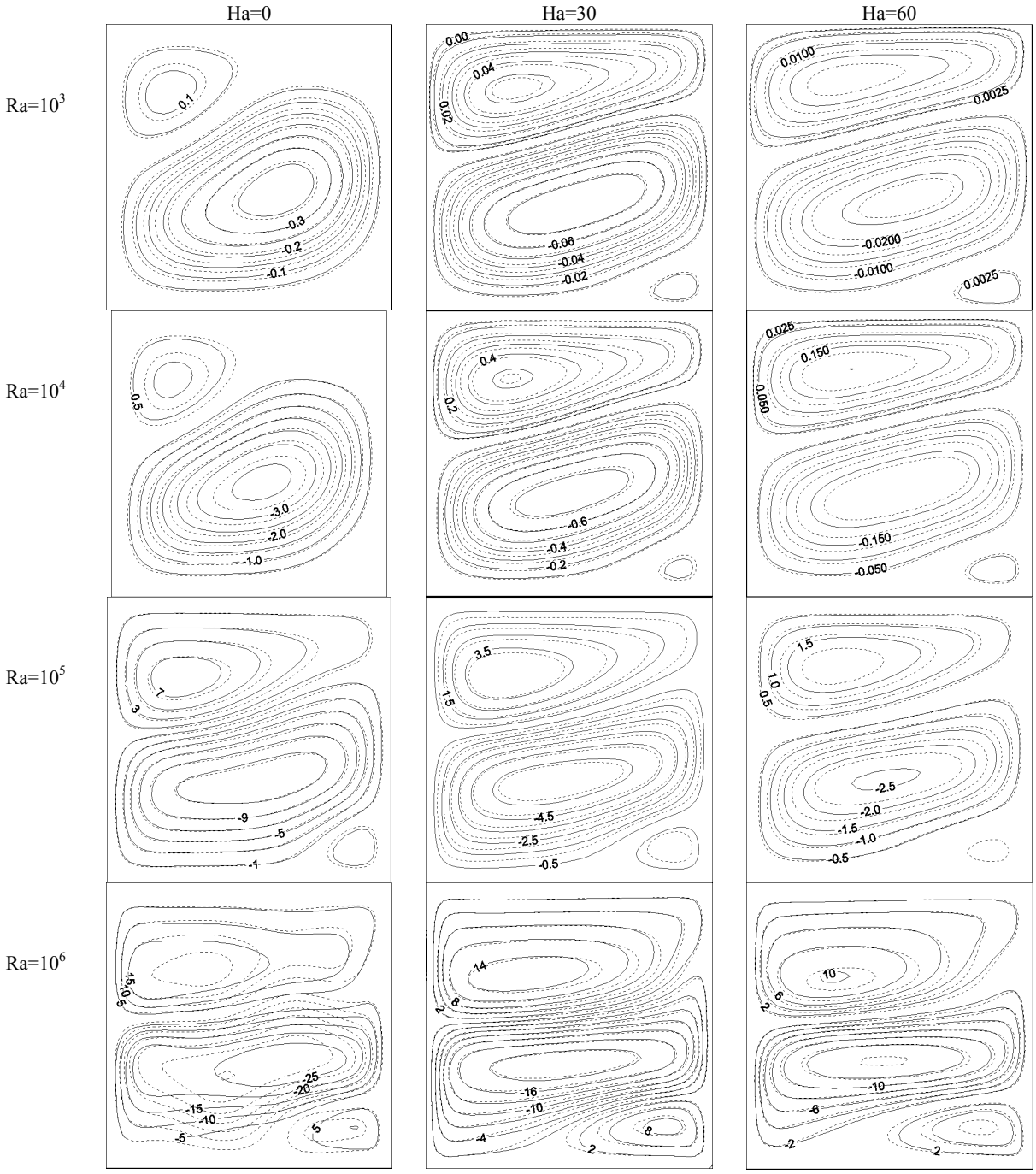

Fig. 7 Streamlines for different Hartmann and Rayleigh numbers and for γ=π/2, (—) $\phi = 0.04$ and (- - -) $\phi = 0$

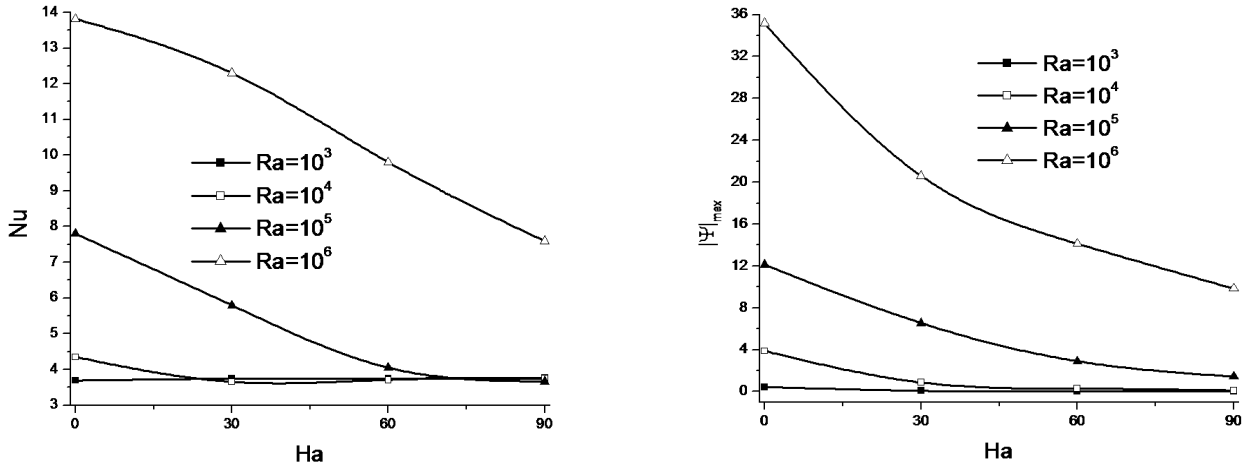

(a) (b)

Fig. 8 Variation of the maximum of the average Nusselt number (a) and stream function (b) with Hartmann number for different Rayleigh number for γ=π/2 and $\phi = 0$

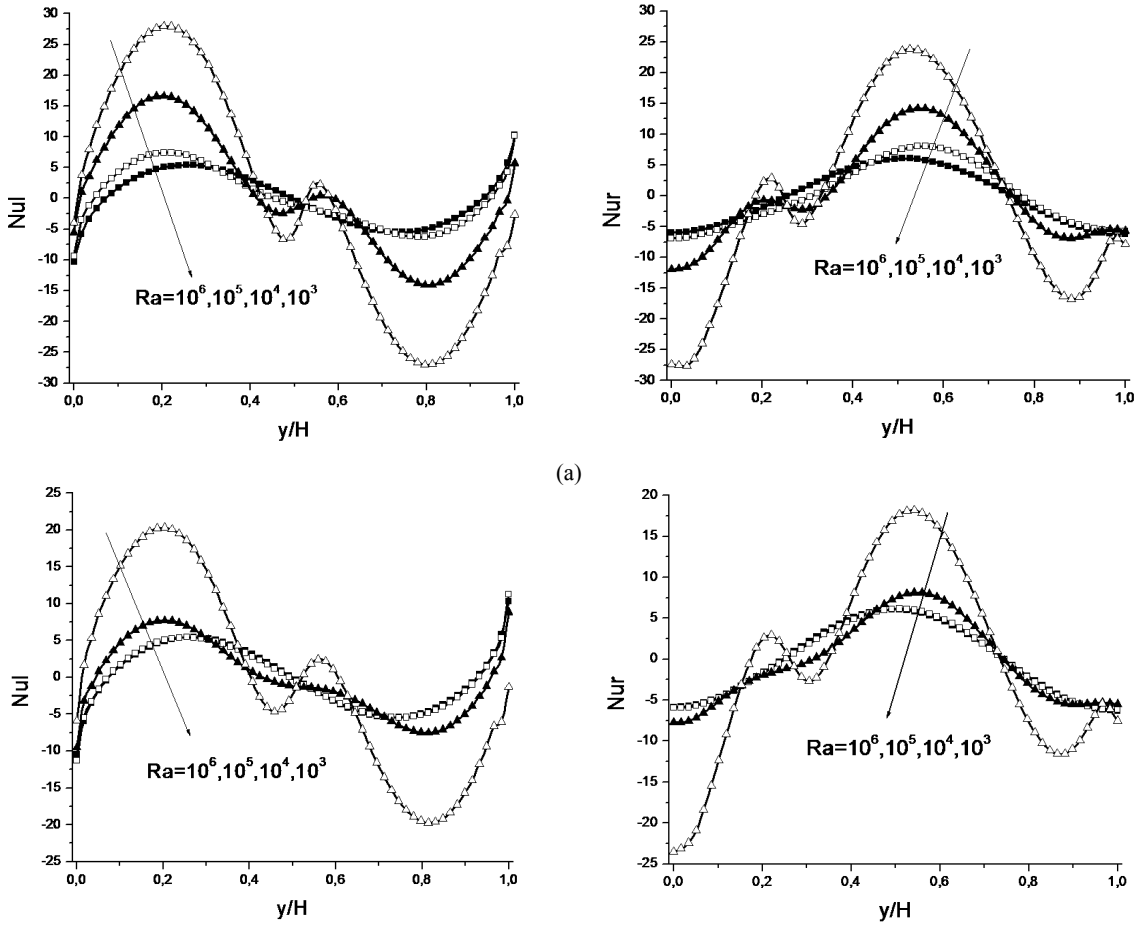

(a)

(b)

Fig. 9 Variation of the local Nusselt number on the left and the right walls for different Rayleigh number for Ha=0 (a) and Ha=60 (b) for γ=π/2 and $\phi = 0$

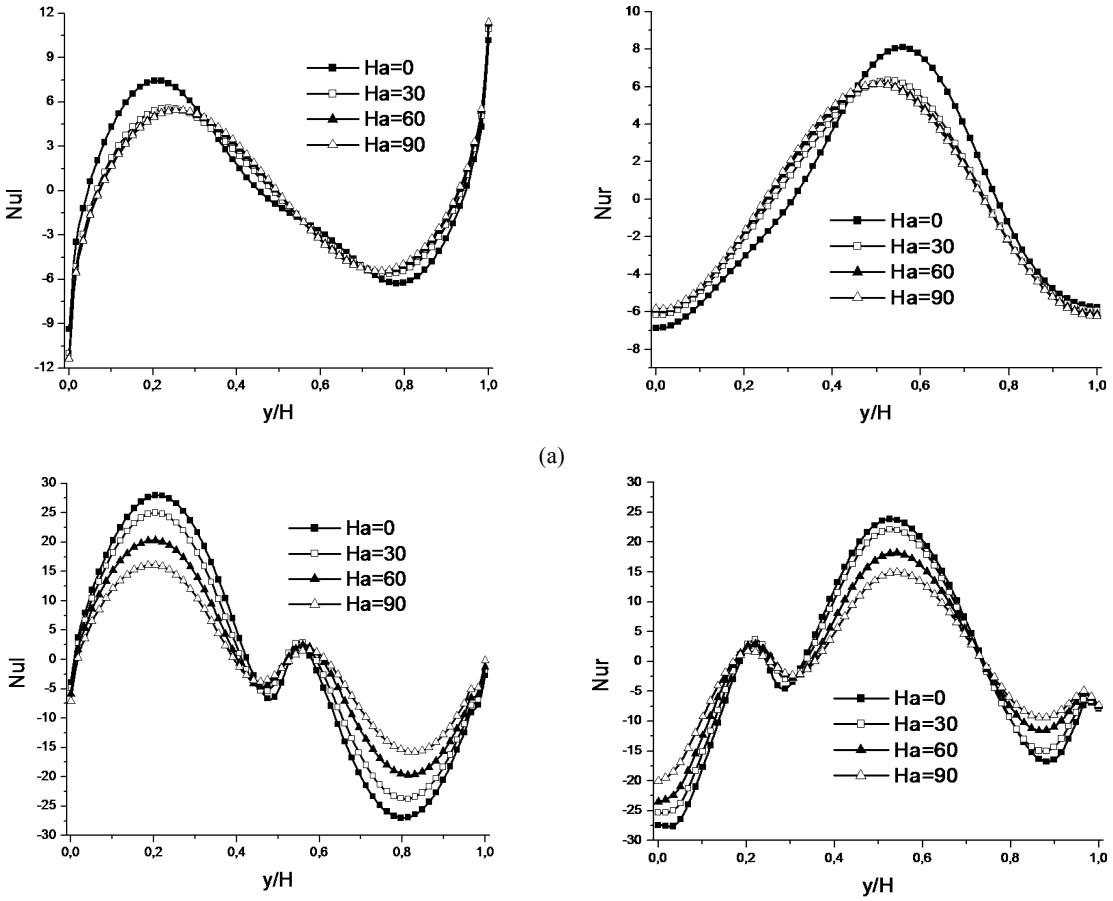

(a)

(b)

Fig. 10 Variation of the local Nusselt number on the left and the right walls for different Hartmann number for Ra=10^4 (a) and Ra=10^6 (b) for γ=π/2 and $\phi = 0$

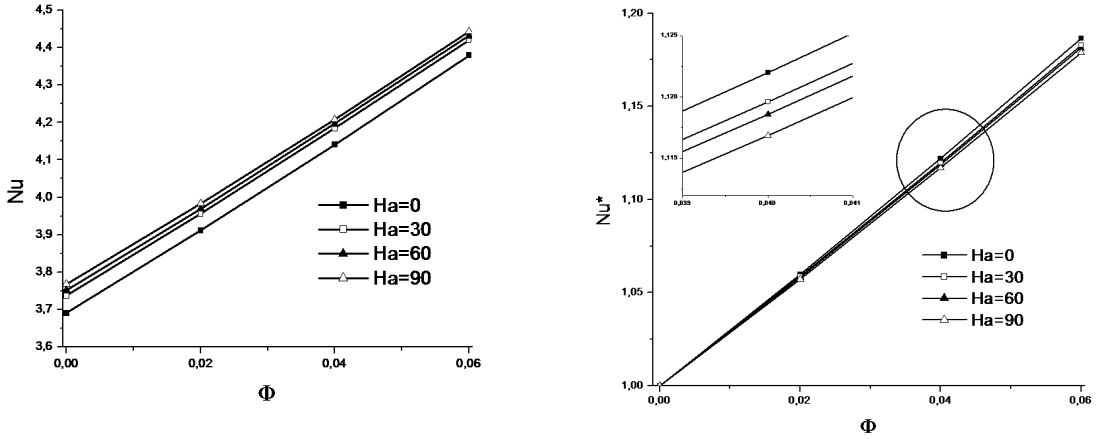

(a)

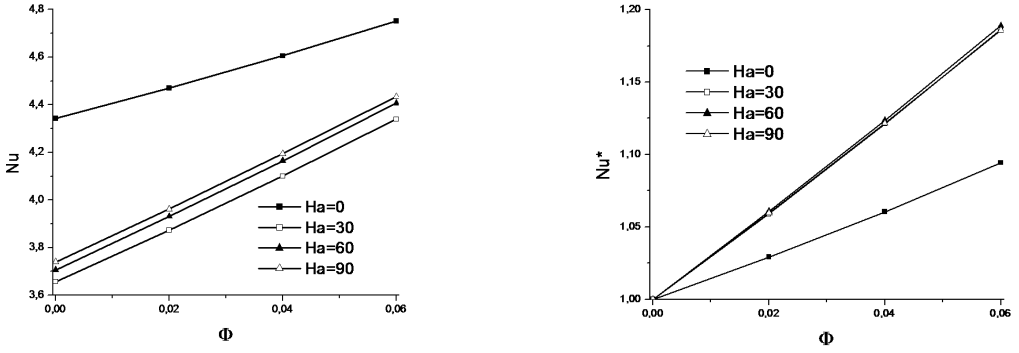

(b)

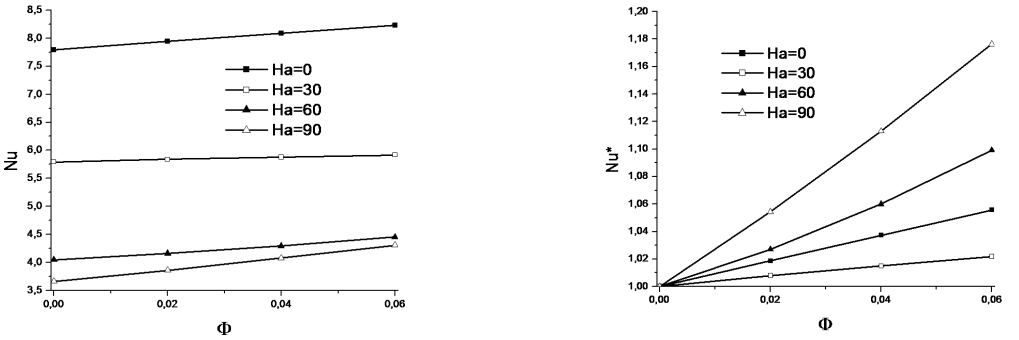

(c)

Fig. 11 Variation of the average Nusselt number and dimensionless average Nusselt number as function of solid volume fraction for different Hartmann number for $\gamma=\pi/2$, $Ra=10^3$ (a) $Ra=10^4$ (b) and $Ra=10^5$ (c)

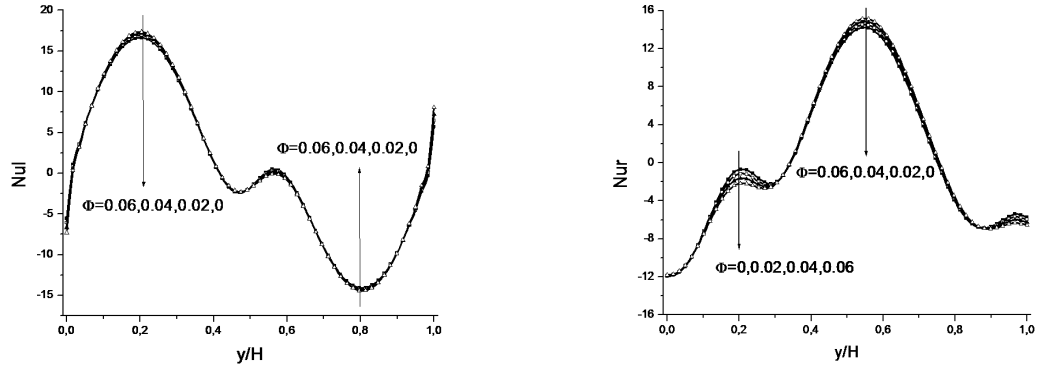

(a)

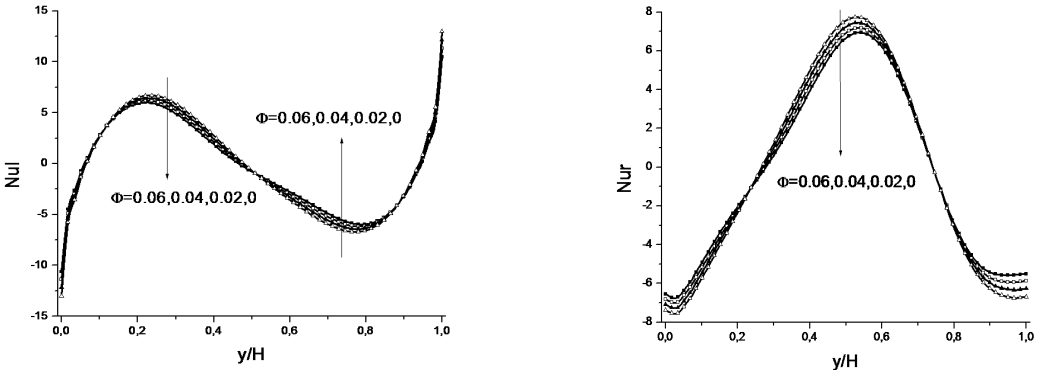

(b)

Fig. 12 Variation of the local Nusselt number on the left and the right walls for different solid volume fraction at $\gamma=\pi/2$, $Ra=10^5$ for Ha=0 (a) and Ha=90 (b)

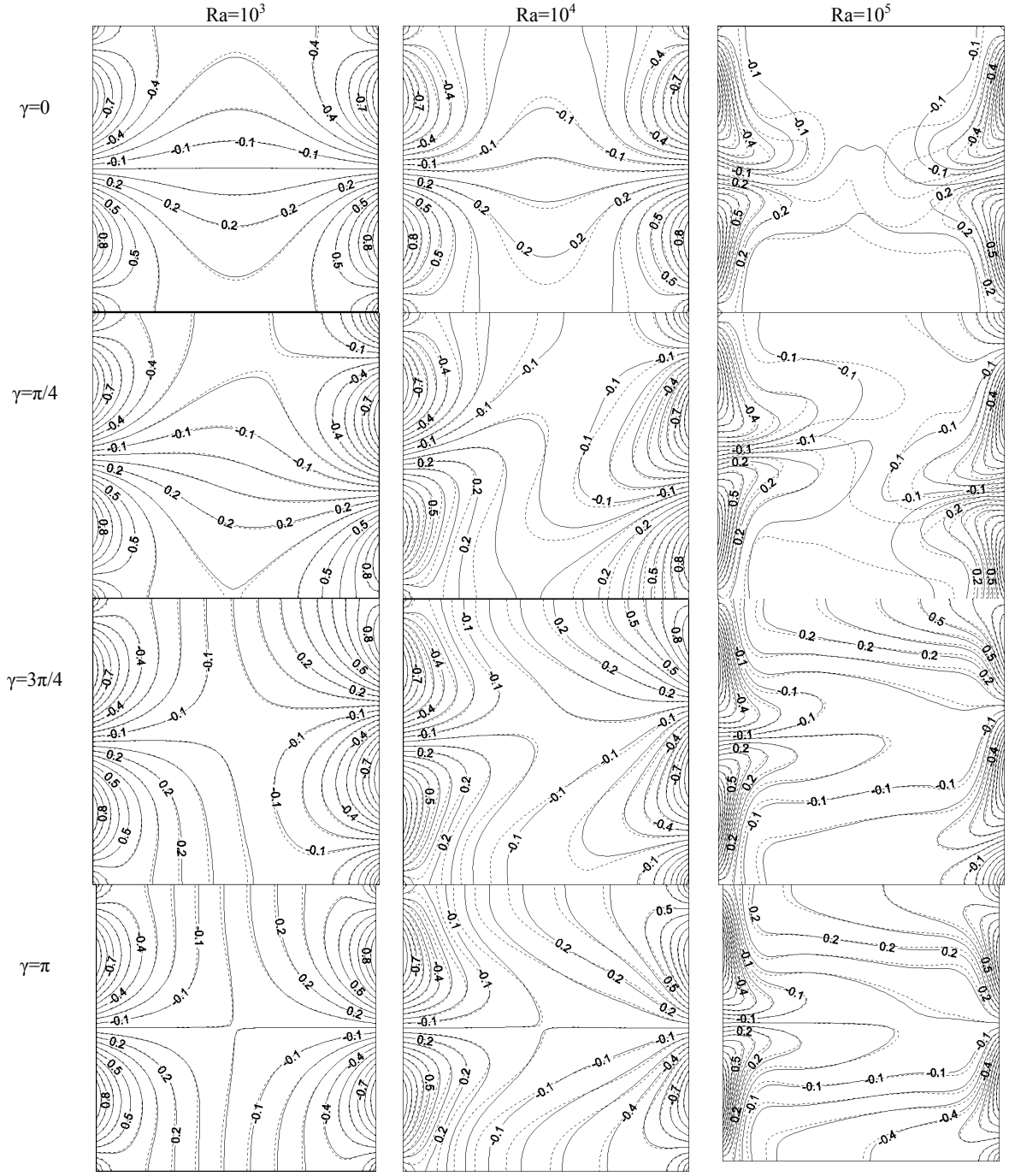

Fig. 13 Isotherms for different Rayleigh number and phase deviations for Ha=0, (—) $\phi = 0.04$ and (- - -) $\phi = 0$

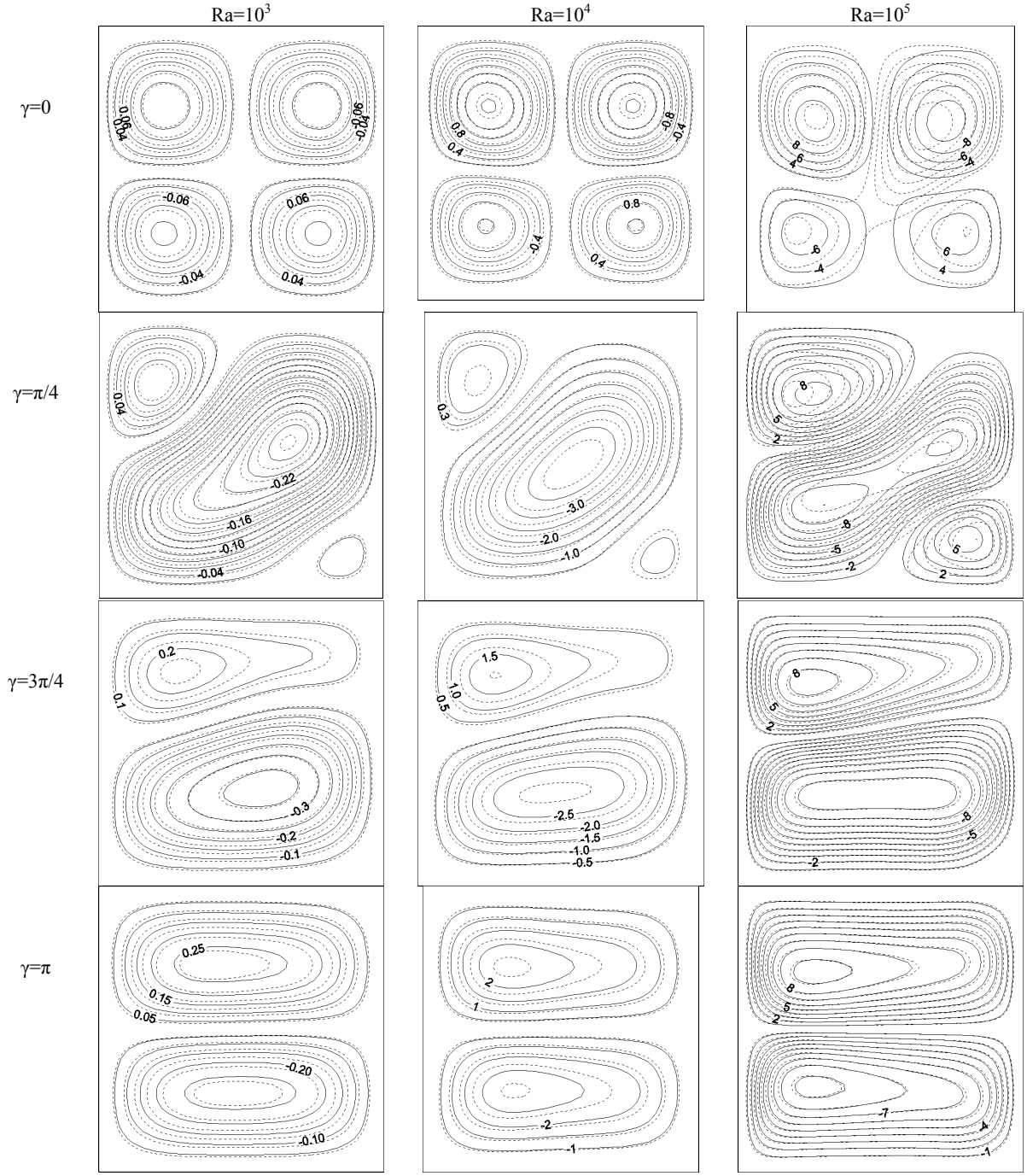

Fig. 14 Streamlines for different Rayleigh number and phase deviations for Ha=0, (—) $\phi = 0.04$ and (- - -) $\phi = 0$

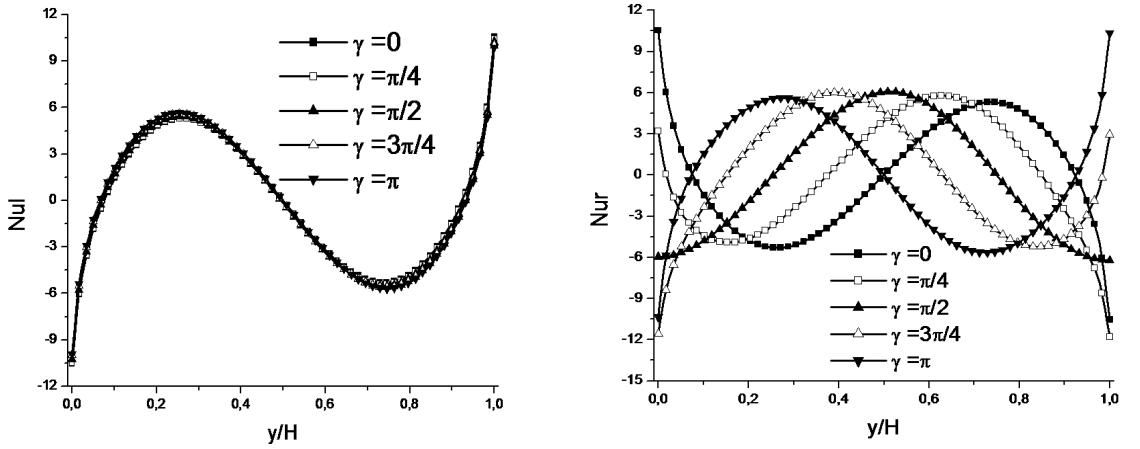

(a)

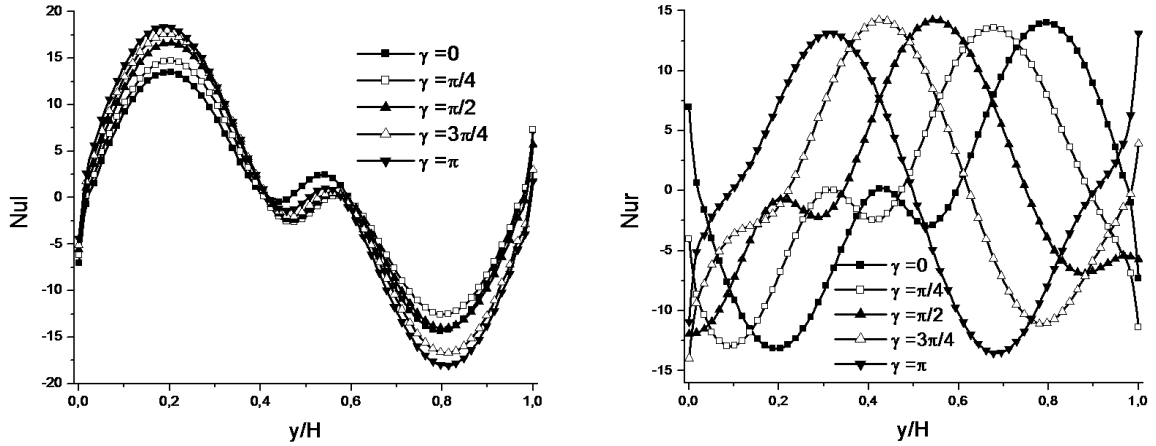

(b)

Fig. 15 Variation of the local Nusselt number on the left and the right walls for different phase deviations at Ha =0 and $\phi = 0$ for Ra=10^3 (a) and Ra=10^5 (b)

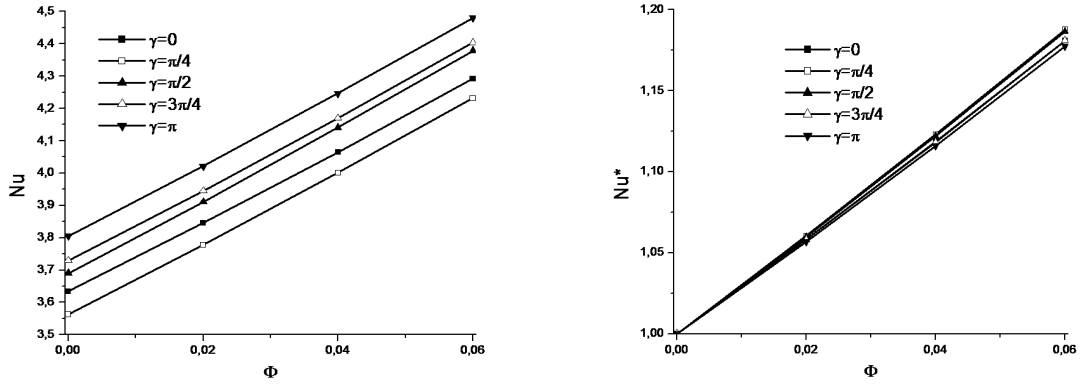

(a)

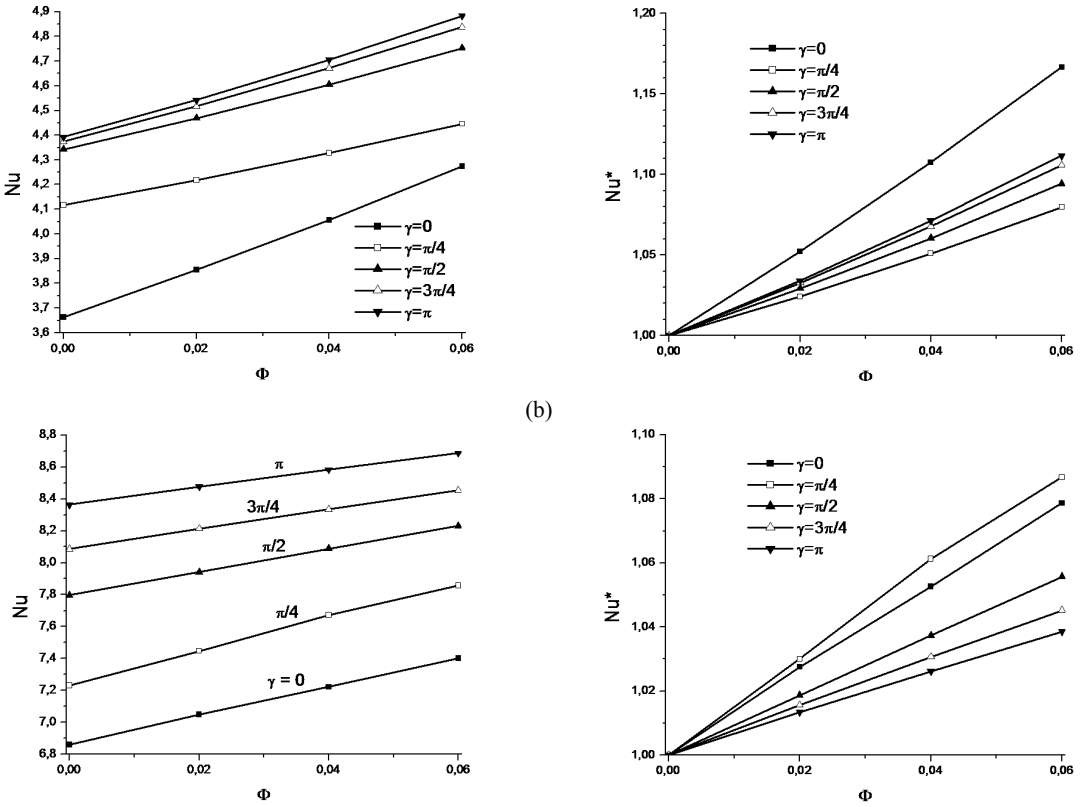

Fig. 16 Variation of the average Nusselt number and dimensionless average Nusselt number as function of solid volume fraction for different phase deviations for Ha=0, $Ra=10^3$ (a) $Ra=10^4$ (b) and $Ra=10^5$ (c)

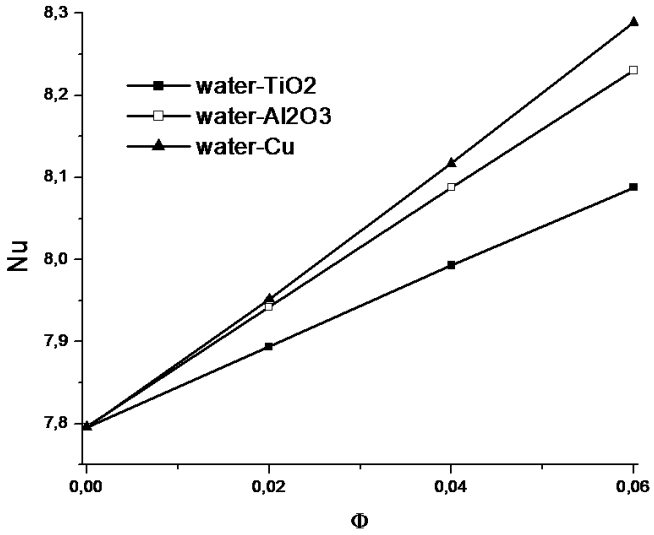

Fig. 17 Comparison between different nanofluids at γ=π/2, Ha =0 and $Ra=10^5$

REFERENCES

[1] S. Ostrach, "Natural convection in enclosures", Journal of Heat Transfer, vol. 110, pp. 1175-1190, 1988.

[2] M. Moreau, "Magnetohydrodynamics", Kluwer Acadamic Publishers, The Netherlands, 1990.

[3] H. Ozoe and K. Okada, "The effect of the direction of the external magnetic field on the three dimensional natural convection in a cubical enclosure", International Journal of Heat and Mass Transfer, vol. 32, pp. 1939-1954, 1989.

[4] J.P. Garandet, T. Alboussiere and R. Moreau, "Buoyancy driven convection in a rectangular enclosure with a transverse magnetic field", International Journal of Heat and Mass Transfer, vol. 35, pp. 741-748, 1992.

[5] M. Venkatachalappa and C.K. Subbaraya, "Natural convection in a rectangular enclosure in the presence of a magnetic field with uniform heat flux from the side walls", Acta Mechanica, vol. 96, pp. 13-26, 1993.

[6] S. Alchaar, P. Vasseur and E. Bilgen, "Natural convection heat transfer in a rectangular enclosure with a transverse magnetic field", Journal of Heat Transfer, vol. 117, pp. 668-673, 1995.

[7] N. Rudraiah, R.M. Barron, M. Venkatachalappa and C.K. Subbaraya, "Effect of a magnetic field on free convection in a rectangular enclosure", International Journal of Engineering Science, vol. 33, pp. 1075-1084, 1995.

[8] K. Khanafer, K. Vafai and M. Lightstone, "Buoyancy-driven heat transfer enhancement in a two-dimensional enclosure utilizing nanofluids", International Journal of Heat and Mass Transfer, vol. 46, pp. 3639-3653, 2003.

[9] K. Kahveci, "Buoyancy driven heat transfer of nanofluids in a tilted enclosure", Journal of Heat Transfer, vol. 132, pp. 062501, 2010.

[10] N. Putra, W. Roetzel and S.K. Das, "Natural convection of nano-fluids", Heat and Mass Transfer, vol. 39, pp. 775-784, 2003.

[11] D. Wen and Y. Ding, "Formulation of nanofluids for natural convective heat transfer applications", International Journal of Heat and Fluid Flow, vol. 26, pp. 855-864, 2005.

[12] M. Pirmohammadi and M. Ghassemi, "Effect of magnetic field on convection heat transfer inside a tilted square enclosure", International Communications in Heat and Mass Transfer, vol. 36, pp. 776-780, 2009.

[13] M.C. Ece and E. Buyuk, "Natural-convection flow under a magnetic field in an inclined rectangular enclosure heated and cooled on adjacent walls", Fluid Dynamics Research, vol. 38, pp. 564-590, 2006.

[14] M. Sathiyamoorthy and A. Chamkha, "Effect of magnetic field on natural convection flow in a liquid gallium filled square cavity for

linearly heated side wall(s)", International Journal of Thermal Sciences, vol. 49, pp. 1856-1865, 2010.
[15] S. Sivasankaran and C.J. Ho, "Effect of temperature dependent properties on MHD convection of water near its density maximum in a square cavity", International Journal of Thermal Sciences, vol. 47, pp. 1184-1194, 2008.
[16] D. Wen and Y. Ding, "Formulation of nanofluids for natural convective heat transfer applications", International Journal of Heat and Fluid Flow, vol. 26, pp. 855–864, 2005.
[17] H.F. Oztop and E. Abu-Nada, "Numerical study of natural convection in partially heated rectangular enclosure filled with nanofluids", International Journal of Heat and Fluid Flow, vol. 29, pp. 1326–1336, 2008.
[18] E. Abu-Nada, "Effects of variable viscosity and thermal conductivity of Al2O3–water nanofluid on heat transfer enhancement in natural convection", International Journal of Heat and Fluid Flow, vol. 30, pp. 679–690, 2009.
[19] E. Abu-Nada, "Effects of variable viscosity and thermal conductivity of CuO–water nanofluid on heat transfer enhancement in natural convection: mathematical model and simulation", ASME Journal of Heat Transfer, vol. 132, pp. 052401, 2010.
[20] E. Abu-Nada, Z. Masoud, H. Oztop and A. Campo, "Effect of nanofluid variable properties on natural convection in enclosures", International Journal of Thermal Sciences, vol. 49, pp. 479–491, 2010.
[21] E. Abu-Nada and A. Chamkha, "Effect of nanofluid variable properties on natural convection in enclosures filled with a CuO–EG–water nanofluid", International Journal of Thermal Sciences, vol. 49, pp. 2339–2352, 2010.
[22] E. Abu-Nada and A. Chamkha, "Mixed convection flow in a lid-driven inclined square enclosure filled with a nanofluid", *European Journal* of Mechanics B Fluids, vol. 29, pp. 472–482, 2010.
[23] Pravez Alam, Ashok Kumar, S. Kapoor and S.R. Ansari, "Numerical investigation of natural convection in a rectangular enclosure due to partial heating and cooling at vertical walls", Communications in Nonlinear Science and Numerical Simulation, vol. 17, pp. 2403–2414, 2012.
[24] E. Fattahi, M. Farhadi, K. Sedighi and H. Nemati, "Lattice Boltzmann simulation of natural convection heat transfer in nanofluids", International Journal of Thermal Sciences, vol. 52, pp. 91-101, 2012.
[25] G.H.R. Kefayati, S.F. Hosseinizaeh, M. Gorji and H. Sajjadi, "Lattice Boltzmann simulation of natural convection in tall enclosures using water/SiO2 nanofluid", International Communications in Heat and Mass Transfer, vol. 38, pp. 798-805, 2011.
[26] F. Lai and Y. Yang, "Lattice Boltzmann simulation of natural convection heat transfer of Al_2O_3/water nanofluids in a square enclosure", International Journal of Thermal Sciences, vol. 50, pp. 1930-1941, 2011.
[27] A.H. Mahmoudi, M. Shahi, A.M. Shahedin and N. Hemati, "Numerical modeling of natural convection in an open cavity with two vertical thin heat sources subjected to a nanofluid", International Communications in Heat and Mass Transfer, vol. 38, pp. 110-118, 2011.
[28] GH. R. Kefayati, M. Gorji, D. D. Ganji and H. Sajjadi, "Investigation of Prandtl number effect on natural convection MHD in an open cavity by Lattice Boltzmann Method", Engineering Computations, vol. 30, pp. 97-116, 2013.
[29] GH. R. Kefayati, M. Gorji, H. Sajjadi and D.D. Ganji, "Lattice Boltzmann simulation of MHD mixed convection in a lid-driven square cavity with linearly heated wall", Scientia Iranica, vol. 19, pp. 1053–1065, 2012.
[30] H. Nemati, M. Farhadi, K. Sedighi , M.M. Pirouz and E. Fattahi, "Numerical simulation of fluid flow around two rotating side by side circular cylinders by Lattice Boltzmann method", International Journal of Computational Fluid Dynamics, vol. 24, pp. 83–94, 2010.
[31] M. Mehravaran and S.K. Hannani, "Simulation of buoyant bubble motion in viscous flows employing lattice Boltzmann and level set methods", Scientia Iranica, vol. 18, pp. 231–240, 2011.
[32] M. M. Pirouz, M. Farhadi, K. Sedighi, H. Nemati and E. Fattahi, "Lattice Boltzmann simulation of conjugate heat transfer in a rectangular channel with wall-mounted obstacles", Scientia Iranica, Transaction B: Mechanical Engineering, vol. 18, pp. 213–221, 2011.
[33] A.A. Mohamad, "Applied Lattice Boltzmann Method for transport phenomena, momentum", Heat and mass transfer, Sure, Calgary, 2007.
[34] S. Succi, "The lattice Boltzmann equation for fluid dynamics and beyond", Clarendon Press, Oxford, London, 2001.
[35] D. Martinez, S. Chen and W.H. Matthaeus, "Lattice Boltzmann magneto hydrodynamics", Physics of Plasmas, vol. 1, pp. 1850–1867, 1994.
[36] H. Nemati, M. Farhadi, K. Sedighi, E. Fattahi and A.A.R. Darzi, "Lattice Boltzmann simulation of nanofluid in lid-driven cavity", International Communications in Heat and Mass Transfer, vol. 37, pp. 1528–1534, 2010.
[37] Y. Xuan and W. Roetzel, "Conceptions for heat transfer correlation of nanofluids", International Journal of Heat and Mass Transfer, vol. 43, pp. 3701-3707, 2000.
[38] H.C. Brinkman, "The viscosity of concentrated suspensions and solution", The Journal of Chemical Physics, vol. 20, pp. 571-581, 1952.
[39] J.C. Maxwell, "A Treatise on Electricity and Magnetism", vol. II, Oxford University Press, Cambridge, UK, 1873, pp. 54.
[40] Q.H. Deng and J. Chang, "Natural convection in a rectangular enclosure with sinusoidal temperature distributions on both sidewalls", Numer. Heat Transfer A, vol. 54, pp. 507–524, 2008.
[41] B. Ghasemi, S.M. Aminossadati and A. Raisi, "Magnetic field effect on natural convection in a nanofluid-filled square enclosure", International Journal of Thermal Sciences, vol. 50, pp. 1748-1756, 2011.
[42] M. Jahanshahi , S.F. Hosseinizadeh , M. Alipanah , A. Dehghani and G.R. Vakilinejad "Numerical simulation of free convection based on experimental measured conductivity in a square cavity using Water/SiO2 nanofluid", International Communications in Heat and Mass Transfer, vol. 37, pp. 687–694, 2010.